Earth and Planetary Science Letters 585 (2022) 117526

Contents lists available at ScienceDirect

Earth and Planetary Science Letters

www.elsevier.com/locate/epsl

# Estimates of paleo-crustal thickness at Cerro Aconcagua (Southern Central Andes) from detrital proxy-records: Implications for models of continental arc evolution

Barbara Carrapa [a,*], Peter G. DeCelles [a], Mihai N. Ducea [a,b], Gilby Jepson [a], Arthur Osakwe [a], Elizabeth Balgord [c], Andrea L. Stevens Goddard [d], Laura A. Giambiagi [e]

[a] Department of Geosciences, University of Arizona, 1040 E 4th St, Tucson, AZ 85721, United States of America
[b] Faculty of Geology and Geophysics, University of Bucharest, 010041, Bucharest, Romania
[c] Earth and Environmental Sciences, Weber State University, 1415 Edvalson St., Ogden, UT 84408, United States of America
[d] Department of Earth and Atmospheric Sciences, Indiana University, 1001 East 10th Street, Bloomington, IN 47405-1405, United States of America
[e] Centro Científico y Tecnológico CCT Mendoza, Av. Ruiz Leal s/n - Parque Gral. San Martín, M5500 Mendoza, Argentina

ARTICLE INFO

*Article history:*
Received 10 November 2021
Received in revised form 19 March 2022
Accepted 29 March 2022
Available online xxxx
Editor: R. Hickey-Vargas

*Keywords:*
Central Andes
crustal thickness
Aconcagua
continental arc
shortening
crustal flow

ABSTRACT

The Central Andes represent the archetypical Cordilleran orogenic system, with a well-developed continental volcanic arc and some of the thickest crust on Earth. Yet the relative contributions of shortening and magmatic additions to crustal thickening remain difficult to quantify, which hinders understanding processes of crustal evolution in continental arcs. Cerro Aconcagua, the highest mountain in the Americas and a relict Miocene stratovolcano resting on 55 km-thick crust, is the ideal natural laboratory to address this issue in subduction-related magmatic arcs because it preserves a multi-million year record of magmatism and deformation within the Aconcagua fold-thrust belt. Estimates of paleo-crustal thickness in the Andes can be made using the geochemistry of subduction-related magmatic rocks, or minerals crystallized within them. This study applies a geochemical proxy approach for crustal thickness estimates to detrital syntectonic deposits of the Santa Maria Conglomerate derived from the Aconcagua stratovolcano to reconstruct paleo-crustal thickness of the Andes at this latitude. Detrital zircon trace-element data from ashes intercalated in the conglomerate, combined with previously published paleo-crustal thickness data, indicate crustal thicknesses of ~35 km ca. 38 Ma and ~44 km ca. 12 Ma, requiring ~11 km of crustal thickening after ca. 12 Ma to achieve present-day crustal thickness of ~55 km. In the absence of significant magmatism since ca. 10 Ma at this location, we show that more than half of the crustal thickening after 12 Ma, corresponding to 2 km of uplift, was achieved by Miocene shortening. Our study also reveals significant differences in crustal thicknesses between the Central Andes and the southern Central Andes which we speculate may be due to southward crustal flow during the last ~20 My.



## 1. Introduction

Understanding the evolution of orogenic crustal thickness through time remains an important open question (Chapman et al., 2015; Ganade et al., 2021), one that is intimately tied to reconstructing elevation throughout geological time. The relative contributions of magmatism (i.e., magmatic additions from the mantle) and shortening to crustal thickening are particularly relevant in Cordilleran-type orogenic systems such as the Andes, with implications for the plate tectonic geochemical cycle and crustal differentiation processes (Turner and Langmuir, 2015), the coupling between lower- and upper-plate processes (Horton, 2018), and the relationships among the arc, forearc and foreland regions (DeCelles et al., 2015). In Cordilleran-type orogens such as the Andes arc magmatism can contribute significantly to crustal thickening and may occur simultaneously with shortening (DeCelles et al., 2015). Although a long-debated issue in Cordilleran-type orogenic systems (Allmendinger et al., 1997; Ramos, 2009a, 2009b; Ramos et al., 1996) the relative roles of shortening and magmatic additions remain unresolved because it is difficult to find case studies where both shortening and magmatism can be deconvolved and quantified. Arc magmatism commonly obliterates

* Corresponding author.
*E-mail address:* bcarrapa@email.arizona.edu (B. Carrapa).

https://doi.org/10.1016/j.epsl.2022.117526
0012-821X/

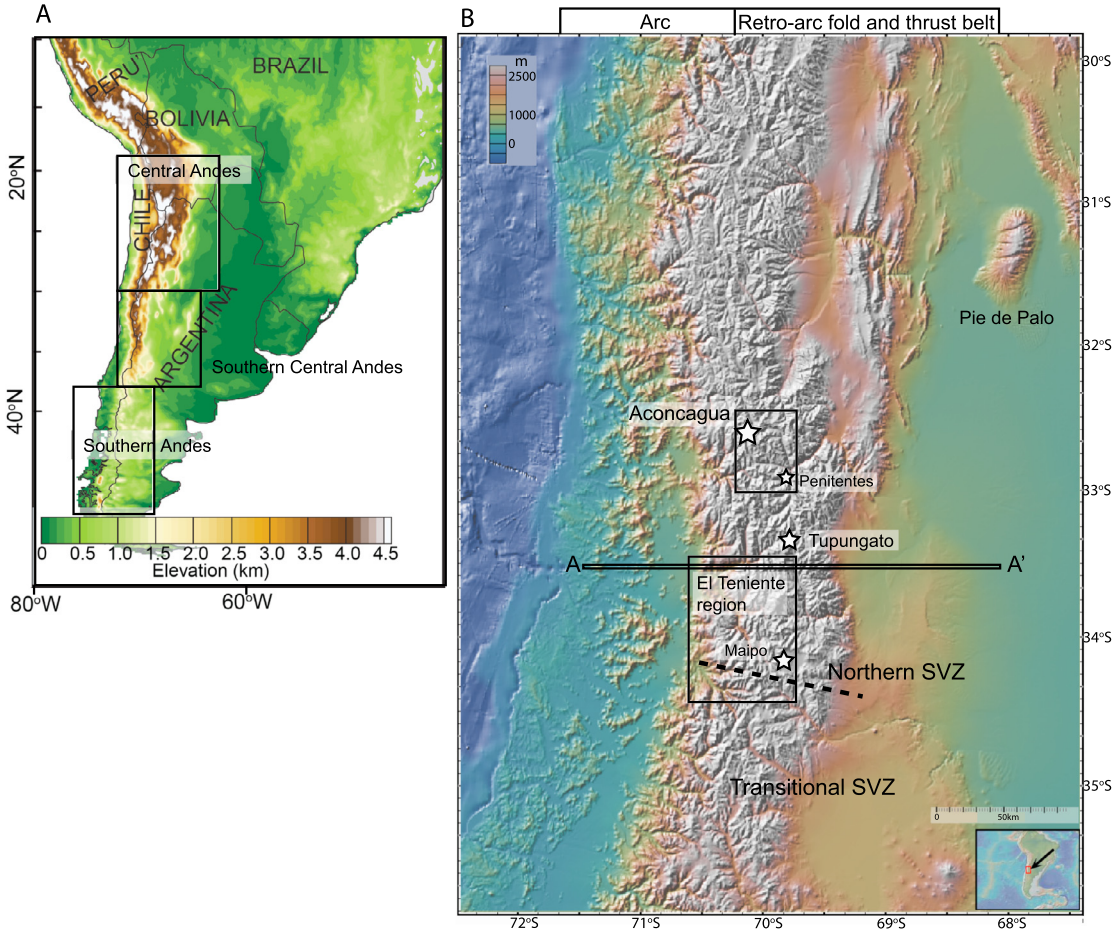


**Fig. 1.** A) Digital elevation model of the Andes; small rectangle outlines the study area shown in Fig. 3, and larger rectangle highlights the El Teniente region discussed in text. A-A' balanced cross section of Giambiagi et al. (2015) used for shortening history in Fig. 7. B) DEM of the southern Central Andes; stars indicate locations of main Miocene and active volcanic centers (Cerros Aconcagua, Maipo, Tupungato) and location of Cerro Penitentes; SVZ: South Volcanic Zone. (For interpretation of the colors in the figures, the reader is referred to the web version of this article.)

earlier records of fold-thrust belt deformation, leaving behind only "ghost" thrust belts that are indirectly constrained and impossible to palinspastically restore (e.g., McQuarrie, 2002). Resolving the timing and relative contributions of deformation and magmatism in crustal evolution is also important for testing tectonic models of Cordilleran-type orogenic systems. For example, periods of flat-slab subduction have been suggested to drive episodic and cyclic behaviors of the Central Andean orogenic system (Kay et al., 2005; Horton, 2018), whereas others suggest that flat-slab subduction is not a necessary requirement to explain the cyclic behavior of the orogenic system (DeCelles et al., 2015).

With an elevation of 6961 m, Cerro Aconcagua in the southern Central Andes of Argentina is the highest mountain in the southern and western hemispheres (Fig. 1). Cerro Aconcagua provides an opportunity to assess crustal thickening through time because it is a former (Miocene) stratovolcano residing in a Miocene to recent fold-thrust belt (Ramos et al., 1996) and hence it is ideally positioned for constraining the timing, origin and relative contribution of crustal thickening using petrochronological methods (Fig. 2). As with most areas in the modern Andes, crustal thickening, up to more than 70 km in places (Beck et al., 1996), occurred mostly over the past 50 Myr, with significant shortening, thickening and uplift over the last ~10 Ma (Hoke et al., 2014a; Giambiagi et al., 2015; Quade et al., 2015). Within that broad constraint, we know that arc magmatism ceased after ~10 Ma in the Cerro Aconcagua area (Ramos et al., 1996). The questions then become: How much crustal thickening took place in the Aconcagua fold-thrust belt be-

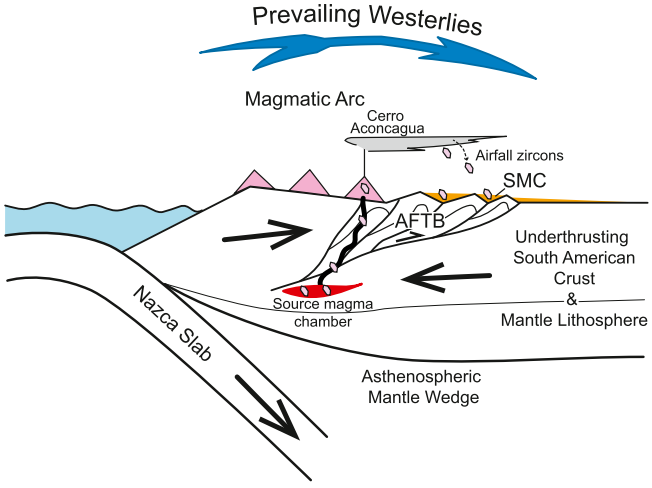


**Fig. 2.** Conceptual cross-section across the western margin of South America, showing the mutual spatial relationships among the Andean magmatic arc, Cerro Aconcagua, the retroarc Aconcagua fold-thrust belt (AFTB), and the Santa Maria Conglomerate (SMC, orange), within the context of converging Nazca and South American plates. Facies, composition, and intra-formational unconformities in the SMC tie it specifically to Cerro Aconcagua and the AFTB. Zircons (small bipyramidal crystals) are crystallized within source magma chambers under pressure-temperature conditions that are mainly controlled by crustal thickness. After transport to the surface they are erupted and distributed eastward across the retroarc region by prevailing westerly winds. Zircons preserved within the SMC provide a long-term record of changing crustal thickness in this region.

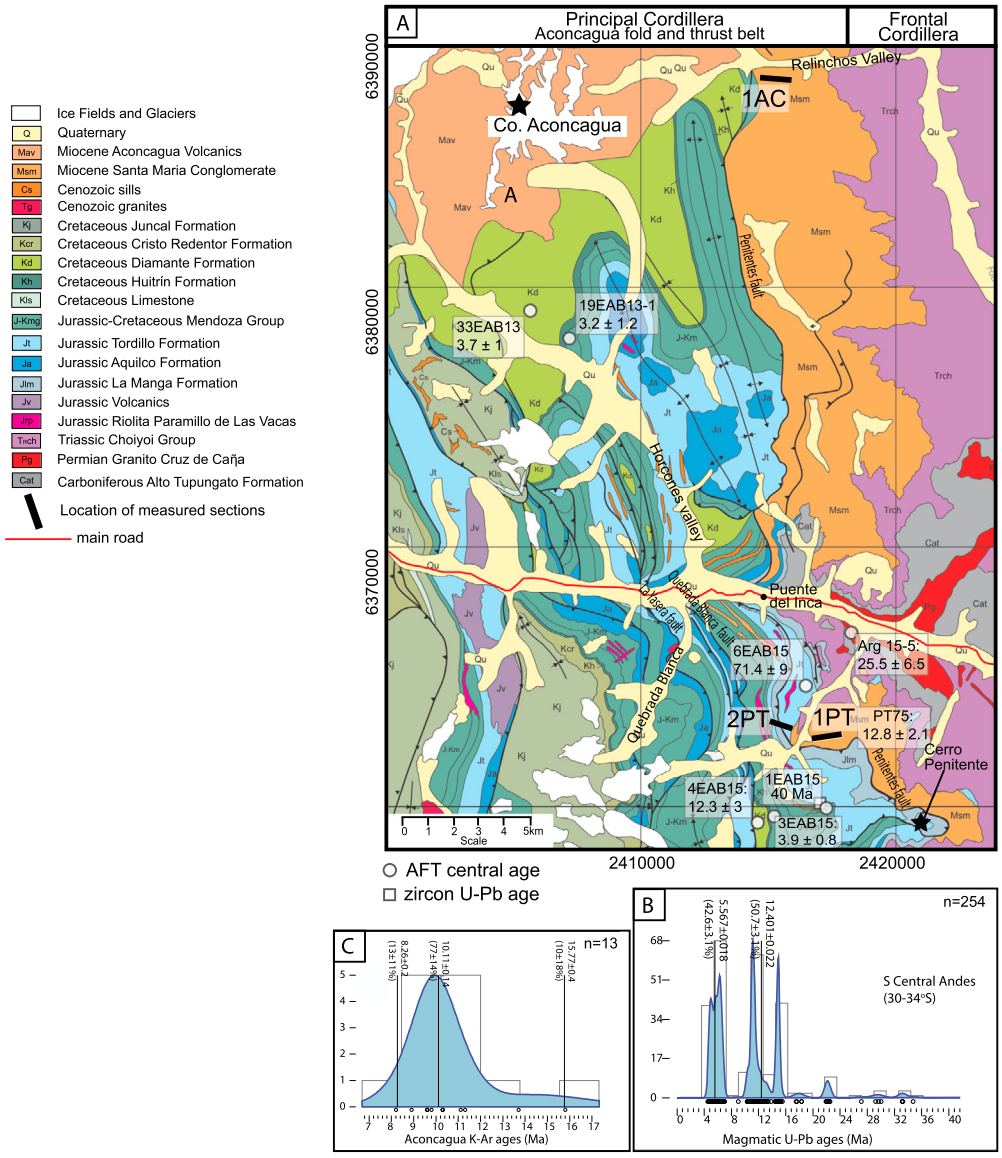


**Fig. 3.** A) Geological map of the study area (modified after Ramos et al. (1996) and Ramos (2009a, 2009b)) with locations of the SMC stratigraphic sections and samples; B) probability density function of magmatic ages for the southern Central Andes after Pepper et al. (2016) (for sample locations see Fig. S3); C) K-Ar ages from the Aconcagua region (Ramos et al., 1996).

fore and after peak magmatism at around 10-12 Ma (Fig. 3B-C)? and what are the relative contributions of magmatism and shortening to crustal thickening? To address these questions we require quantitative constraints on past crustal thickness (Balica et al., 2020; Profeta et al., 2015; Tang et al., 2020) and the shortening history at the same locality. The Cerro Aconcagua area provides all of the requisite features for such an analysis.

Here we present a multi-disciplinary study applied to Miocene synorogenic deposits (Santa Maria Conglomerate) near Cerro Aconcagua, with the goal of reconstructing the long time record of magmatism, deformation and crustal thickness at this location and the relationships between the arc and the fold-thrust belt (Fig. 2). In this study, we use a technique based on magmatic zircons from Middle Miocene tuffs and detrital co-magmatic and inherited zircons, as well as whole-rock geochemical data, to reconstruct crustal thicknesses in the Aconcagua region since the Eocene. Paleo-crustal thickness calculations based on co-magmatic zircon geochemical data indicate a "normal" baseline crustal thickness of ~35 km at ca. 38 Ma and ~44 km ca. 12 Ma. Our data show that a significant amount of thickening took place before and after peak magmatism (~12-10 Ma) with more than half of the crustal thickening occurring after ca. 12 Ma during continued development of the Aconcagua fold-thrust belt. Our findings demonstrate that thick crust, which occurs where the frontal arc of the Andean Cordillera achieves its highest elevation, is largely controlled by structural shortening.

## 2. Geological setting

The Central Andes form the highest mountains in the American Cordilleras and are underlain by some of the thickest crust on Earth (up to 74 km; Beck et al., 1996). They include a high elevation "frontal" volcanic arc to the west and a retroarc fold-thrust belt to the east. The fold-thrust belt is divided into the Principal Cordillera, Frontal Cordillera, and Precordillera (Fig. 3) (e.g., Giambiagi et al., 2015). Cerro Aconcagua is located in the Principal Cordillera (Fig. 3), ~50 km north of Cerro Tupungato, the northernmost volcano of the active Southern Volcanic Zone (SVZ; Fig. 1B) (Hildreth and Moorbath, 1988). Cerro Aconcagua also lies within the Aconcagua fold-thrust belt (Fig. 3), which was deform-

ing between ~18 and 5 Ma (Giambiagi et al., 2015). Exhumation of the Frontal Cordillera occurred as early as 25-20 Ma (Hoke et al., 2014b; Riesner et al., 2019).

Along a transect through the Aconcagua region from the offshore Chilean trench to the continental interior arc, magmatism generally migrated eastward during Mesozoic and Cenozoic time. Magmatism was interrupted during the Oligocene, but restarted during latest Oligocene through Miocene time; no magmatism has occurred since ~8 Ma along this transect, and the majority of dated volcanic rocks are older than or equal to ~10 Ma (Fig. 3B-C). Arc migration was presumably related to shallowing of the Nazca slab and freezing of the mantle wedge under the main Andean range at this latitude (Ramos, 2009a, 2009b and references therein). The Aconcagua fold-thrust belt continues southward into the active SVZ (Hildreth and Moorbath, 1988; Kay et al., 2005), where volcanism has continued unabated from the Miocene to the present (Sruogaa et al., 2005). There, the modern stratovolcanoes of Cerros Tupungato, Tupungatito, Marmoleja, San Jose and Maipo are built on top of Pliocene volcanic products and the crust is ~45 to 54 km thick (Gans et al., 2011).

Cerro Aconcagua consists of remnants of a ~15-10 Ma composite stratovolcano, dominated by andesitic and dacitic breccia, porphyritic dacites, andesites and tuffs known as the Aconcagua Volcanic Complex, which is divided into lower (~15.8 – 11.3 Ma) and upper (~11.1 to ~8.2 Ma, but mostly pre 10 Ma) units separated by an angular unconformity (Ramos et al., 1996). In places the Aconcagua Volcanic Complex sits on top of Early Miocene (~21.6 Ma) Matienzo granodiorite. Early to Middle Miocene (~21-15 Ma) shallow intrusive and volcanic rocks are common directly west of Cerro Aconcagua (Ramos et al., 1996), where they were emplaced onto (or intruded into) the upper Cretaceous Juncal Formation (Mackaman-Lofland et al., 2019).

The Miocene Santa Maria Conglomerate (SMC) is a >1000 m thick conglomerate that rests unconformably on the Triassic-Jurassic section in the Cerro Penitentes area and on Permian basement and Triassic Choiyoi Group in areas to the north; it is generally located in the footwall of the west-dipping Penitentes thrust system, which is the easternmost major thrust in the Aconcagua fold-thrust belt (Figs. 3, 4A) (Vicente and Leanza, 2009; Martos et al., 2022). Some workers have divided these deposits into the Penitentes (early Miocene; ~15 Ma) and Santa Maria (late Miocene; ~12-8 Ma) conglomerates mostly based on their interpreted ages (Vicente and Leanza, 2009; Martos et al., 2022); for simplicity we use the single term Santa Maria Conglomerate. The SMC records the timing of deformation of the Aconcagua fold-thrust belt in relation to arc magmatism. However, available ages are sparse and poorly constrained (Martos et al., 2022).

## 3. The Santa Maria Conglomerate as a record of tectonics and magmatism

The SMC is well exposed in the Cerro Penitentes area and to the east and southeast of Cerro Aconcagua, along the border between the Principal and Frontal Cordilleras (Figs. 1, 3A). We measured three stratigraphic sections: 1PT and 2PT in the upper and lower parts of the unit near Cerro Penitentes ~27 km SE of Cerro Aconcagua, and 1AC ~9 km directly east of Cerro Aconcagua on the south side of the Relinchos Valley (Fig. 3A). All measured sections are in the footwall of a thrust fault that juxtaposes hanging-wall Mesozoic strata on footwall Miocene conglomerate (Figs. 3A, 4A, B). Lithofacies codes and associations follow (Smith, 1986), (DeCelles et al., 1991), and (Miall, 2006). Samples are listed in Table S1 and Figure S1 and interpretations of processes and depositional environments are based on lithofacies associations following Table S2.

The SMC is ~1250 m thick at Cerro Penitentes (sections 2PT and 1PT; Figs. 3 and S1), sits in low-angle unconformity upon the Triassic Choiyoi Group (Fig. 4C), and contains internal open folds and evidence of intraformational angular unconformities and minor faults indicative of syn-depositional deformation (Fig. 4E) (see also Vicente and Leanza, 2009; Martos et al., 2022). Bedding in the conglomerate is horizontal to gently westward dipping. Section 2PT is dominated by poorly sorted, massive clast-supported conglomerate (Gcm), with occasional horizontally stratified (Gch), imbricated (Gcmi/Gchi), and massive matrix-supported (Gmm) beds intercalated with massive to horizontally stratified sandstone layers (Sm and Sh) (Fig. 5A, B). Boulder beds composed of >50 cm diameter clasts are common (Fig. 5A). The association of lithofacies Gmm and Gcm suggests deposition by matrix- and clast-rich debris flows and hyperconcentrated flood flows (Nemec and Steel, 1984; Smith, 1986). The association of Gch and Gcmi/Gchi and massive to horizontally stratified sandstone (Sm/Sh) layers suggests deposition by traction transport in less-concentrated, turbulent stream flows.

Section 1PT, which lies conformably above section 2PT, is characterized by facies similar to those observed in 2PT but also includes clast-supported conglomerate with low-angle planar (Gcp) and trough cross-strata (Gct) and beds of horizontally stratified sandstone (Sh). This facies association suggests deposition by turbulent stream flows. Thin beds of lithofacies Fsl occur throughout this section suggesting suspension settling in ponds and ephemeral channels. The coarse grain-size, generally thick bedding, great thickness (>1000 m) and association of both stream-flow and sediment-gravity-flow deposits indicates that the SMC in the Cerro Penitentes outcrops was deposited in an alluvial-fan system (Nemec and Steel, 1984).

Section 1AC is 400 m thick (Figs. 3A and S1) and located along strike to the north of Cerro Penitentes, in the footwall of the same thrust system near Cerro Aconcagua (Figs. 3, 4A). In the Relinchos Valley (Fig. 3A) the conglomerate rests unconformably upon redbeds of the Choiyoi Group and bedding is approximately horizontal (Fig. 4E). Conglomeratic lithofacies in section 1AC (Fig. 5C-F) consist predominantly of dark- to light-gray, poorly sorted, disorganized, clast- and matrix-supported, pebble- to boulder-conglomerates (Gcm and Gmm) with local horizontal stratification (Gch) (Table S2). Inverse- and inverse-to-normal grading is common in beds of Gcm (Fig. 5E). Thick layers of massive to horizontally stratified volcaniclastic sandstone (Sm, Sh) and ash layers (Fig. 5D, E) are common. A ~6-12 m-thick channel-filling columnar jointed andesitic flow unit is present in the upper part of the measured section (Figs. 4F, 5C). The lithofacies association in section 1AC (Table S2) is interpreted to represent deposits of volcanogenic debris flows and hyperconcentrated flood flows (e.g., Smith and Lowe, 1991; Smith, 1986; Cronin et al., 1999) that originated as lahars. The deposits covered at least 125 $km^2$, suggesting that they accumulated in a radially outward sloping volcanogenic alluvial ring-plain that surrounded the Cerro Aconcagua stratovolcano (e.g., Cronin et al., 1999).

Data from imbricated clasts (Figs. 5B, S1) show paleocurrent directions ranging from NNW-ward to SE-ward. Conglomerate clast-count data from measured sections 1PT and 2PT indicate a provenance from Mesozoic limestone, sandstone and Cenozoic magmatic rocks located west of the study area (Fig. S1), consistent with paleocurrent data. Martos et al. (2022) noted the presence of abundant Triassic Choiyoi Group clasts in SMC outcrops south of Cerro Penitentes and interpreted these as a product of erosion in the Frontal Cordillera and westward transport into the SMC depocenter; this is consistent with the fact that the SMC rests in erosional unconformity upon Triassic and Jurassic rocks of the Frontal Cordillera. Compositions of the volcanic clasts suggest a predominantly felsic to intermediate source (dacite, rhyolite and andesite) with limited contributions from basaltic sources. The SMC in section 1AC is

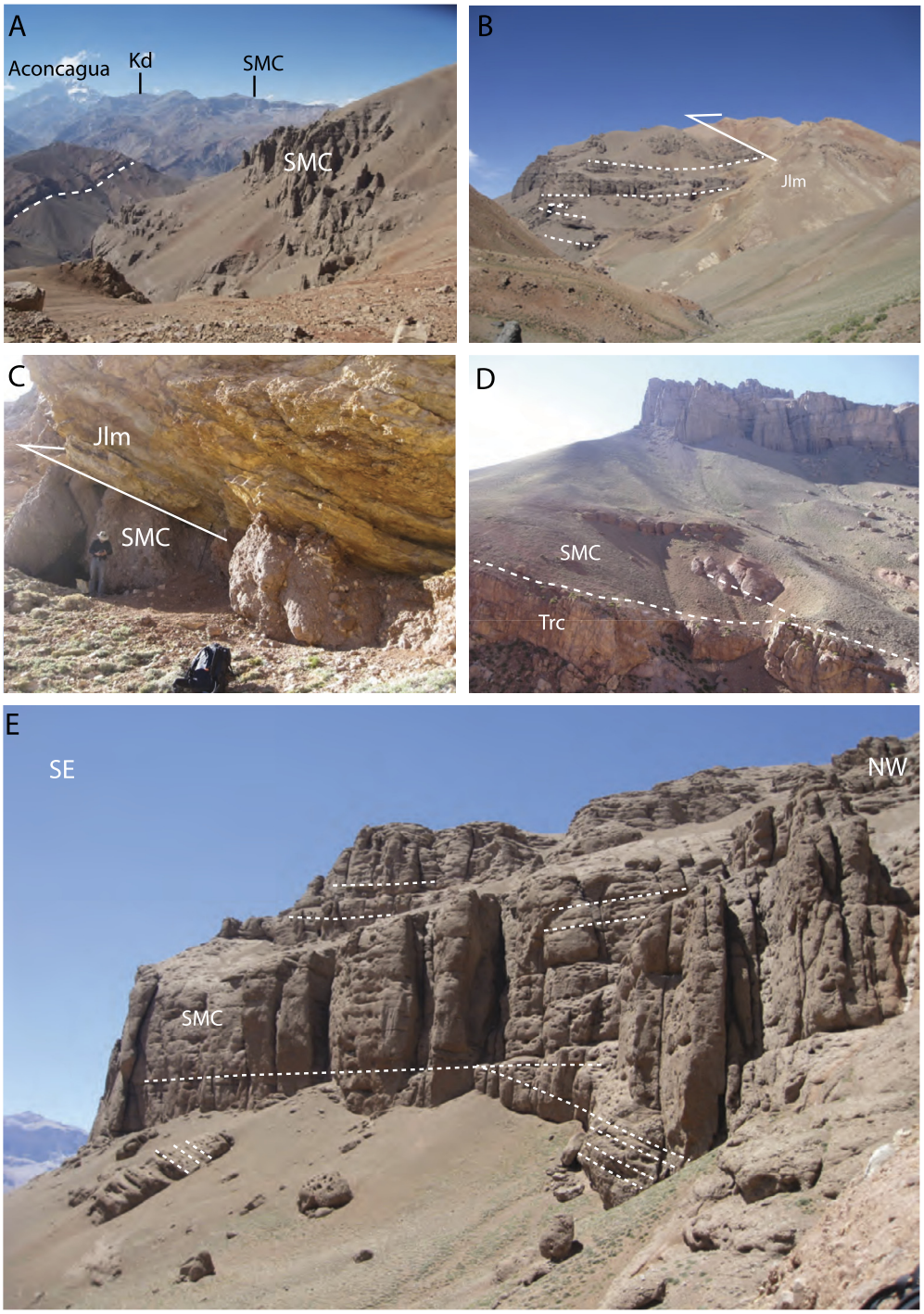


**Fig. 4.** Field photographs of SMC in the Cerro Penitentes and Cerro Aconcagua areas. (A) Northward panorama from Cerro Penitentes with south face of Cerro Aconcagua in upper left, Jurassic La Manga Formation (Jlm) in hanging-wall of the Penitentes thrust in foreground and ledges above the thrust (dashed white line), pinnacled cliffs of sub-horizontal SMC in the middle distance (center-right) structurally beneath the thrust, and Mesozoic rocks (Mz) of the Aconcagua fold-thrust belt in the background, including Cretaceous Diamante Formation (Kd) in core of open syncline in thrust contact on top of the SMC. (B) View southeast of Penitentes thrust, juxtaposing white sandy limestone of Jlm in hanging wall with footwall SMC. (C) Close-up view of the Penitentes thrust. (D) View southeast of basal angular unconformity (white line) separating SMC from Triassic Choiyoi Group (Trc). (E) Intraformational angular uniformities within the SMC. Dashed lines highlight geometric relationships.

mostly composed of clasts (up to boulder size) of andesite, dacite and rhyolite that were most likely derived from Cerro Aconcagua (Fig. S2).

## 4. U-Pb geochronology

Five ash beds and two detrital (one reworked ash) samples were collected from the SMC in the Aconcagua region for zircon U-Pb geochronology (Tables S1, S3; Fig. 6). Analyses were conducted at the Arizona LaserChron Center following procedures described by (Pepper et al., 2016). In addition, one sample from a sill intruded into the Lower Cretaceous Agrio Formation in a thrust sheet within the Aconcagua fold-thrust belt (Fig. 3) was collected (1EAB15) for both zircon U-Pb and apatite fission track (AFT) dating (discussed below). Depositional ages of ash beds and detrital samples were calculated using the TuffZirc Age algorithm

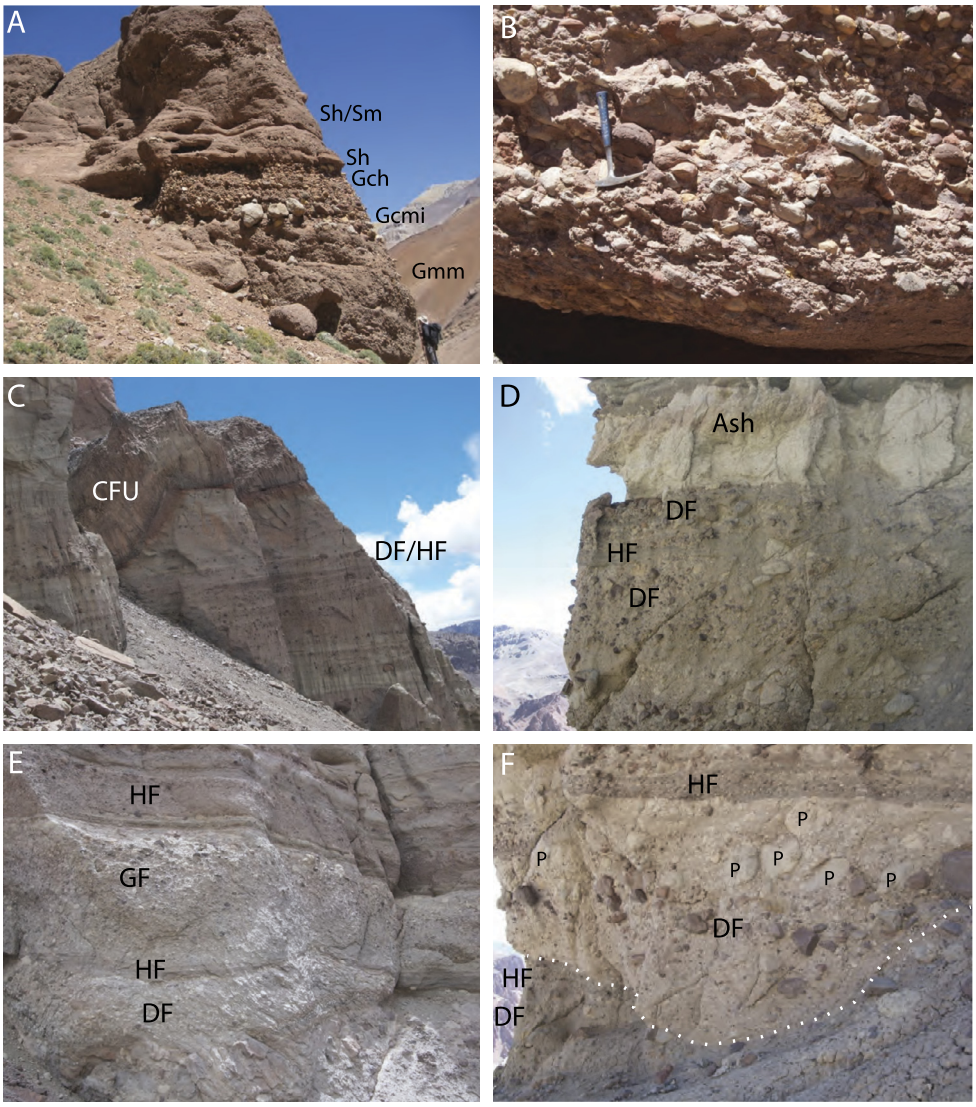


**Fig. 5.** (A) Lithofacies Gmm, Gcmi, Gch, and pebbly-cobbly Sh/Sm in Cerro Penitentes section. (B) Lithofacies Gcmi in Cerro Penitentes section, with clast imbrications indicating eastward (toward the left) paleoflow direction. Hammer is 40 cm long. (C) Erosional channel wall in upper part of measured section 1AC; erosional relief is ~6 m, cutting interbedded debris flow (DF) and hyperconcentrated flood flow (HF) units. Channel is filled with columnar jointed flow unit (CFU). (D) White ash-rich silty sandstone overlying 1.5 m thick lithofacies Gmm and pebbly Gch units interpreted as debris flow (DF) and hyperconcentrated flood flow (HF) deposits. (E) ~1 m thick, inversely graded Gcm unit interpreted as a shear-modified grainflow (GF), with weakly horizontally stratified hyperconcentrated flood flow (HF) lithofacies Sm/Gcm and pebbly to cobbly Gmm lithofacies interpreted as debris flow deposits (DF). (F) Inverse to normally graded unit of Gmm overlying irregular erosional basal surface (white dotted line), interpreted as debris flow unit (DF); note concentration of less dense pumice clasts (some labeled P) in upper half of the ~1.2 m thick bed. The basal erosional surface of this bed cuts underlying hyperconcentrated flood-flow (HF) and debris flow deposits (DF).

by (Ludwig and Mundil, 2002). Most individual zircon ages from the ashes intercalated in the SMC are between ~12 and ~11 Ma. (Table S3; Fig. 6). Sample 1PT171 (a reworked ash) contains a significant component of young zircon grains of ca. 14 Ma. Sample 2PT10 (sandstone) contains Proterozoic through Cenozoic ages (Table S3) with a youngest (Andean) age component of ca. 42 Ma (Table S3; Fig. 6). The close similarities of ages of the SMC at Cerro Penitentes (2PT and 1PT samples) and the volcaniclastic rocks at Cerro Aconcagua (1AC samples) indicate that these deposits are coeval; moreover, the SMC in general was being deposited while the Cerro Aconcagua stratovolcano and the Aconcagua fold-thrust belt were active. The Eocene detrital zircon ages from sample 2PT10 are consistent with the ca. 40 Ma age from the Agrio Formation sill located in the Aconcagua fold-thrust belt (1EAB15). These ages are interesting because they are the first evidence of Eocene magmatic activity in the study area during a time of regional magmatic lull (Haschke et al., 2002).

## 5. Thermochronology

Apatite Fission Track (AFT) thermochronology was applied to samples from the Santa Maria Conglomerate and from different basement lithologies in the Aconcagua fold-thrust belt (Fig. 3) to determine the timing of cooling associated with erosion and deformation. Eight samples from the region between Cerros Aconcagua and Penitentes were analyzed for AFT thermochronology (Fig. 3; Tables S1, S4), following methods and procedures described by (Stevens Goddard and Carrapa, 2017). Sample Arg-15-5 is from a Permian granite that intrudes the Carboniferous section in the footwall of the Penitentes thrust ~4 km north-northeast of Cerro Penitentes (Fig. 1B) and produced a central AFT age of 25.5 ± 6.5 Ma. Four samples from Mesozoic sedimentary units (19EAB13, 33EAB13, 3EAB15, 4EAB15; Table S1) record mostly Miocene and Pliocene ages. Sample 1EAB15 from the Eocene sill cutting through the Cretaceous Agrio Formation, records an age consistent with the

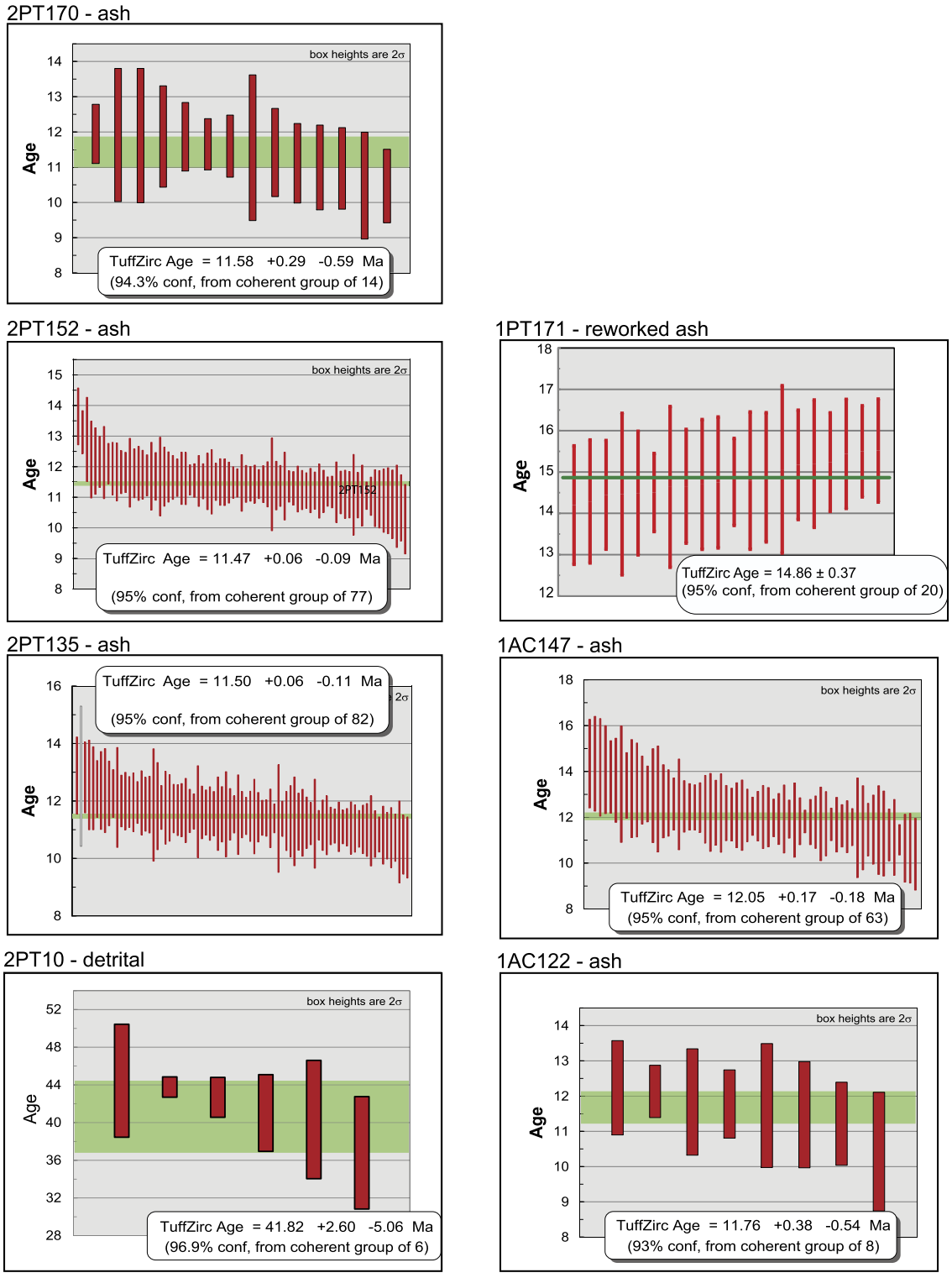


**Fig. 6.** Zircon U-Pb ages and TuffZirc ages from ashes within the Santa Maria Conglomerate (from data in Table S3). For details on sample locations within the measured stratigraphic logs refer to Figure S1.

crystallization age of the sill, and sandstone sample 6EAB15, from the Jurassic Tordillo Formation, records a late Cretaceous age (~71 Ma). Sample 1PT75 is a clast of Jurassic red sandstone from the Santa Maria Conglomerate at Cerro Penitentes and produced an AFT central age of 12.7 ± 2.1 Ma.

We interpret the Miocene AFT ages from the SMC to represent cooling related to source erosion rather than cooling following sediment burial or magmatism based on the following lines of evidence: 1) the thickness of the SMC (~1.2 km) is not enough to have reset the AFT system after deposition, and 2) if the age reflects cooling following Miocene magmatism we would expect nearby basement samples to have been reset as well. The close similarity of the depositional age of the PT sections (~12-11 Ma) and the AFT age of sample 1PT75 (a Jurassic red sandstone clast) requires a very brief lag time, implying rapid erosion of the Aconcagua fold-thrust belt consistent with cooling ages in

the rocks west of the PT sections (sample 4EAB15). The ~25 Ma age (sample Arg-15-5) coincides with early Miocene exhumation of the Frontal Cordillera and suggests that whole orogenic system was internally deforming at this time. The ~71 Ma age from the Jurassic Tordillo Formation (6EAB15) may indicate exhumation of the fold-thrust belt during the late Cretaceous consistent with Cretaceous syn-orogenic deposits of the Diamante Formation (Mackaman-Lofland et al., 2019).

## 6. Detrital zircon petrochronology

Zircons from three ash samples (2PT170, 2PT152, and 2PT135) were analyzed for trace elements simultaneously with age determination via Element 2 high resolution ICPMS with an E2 excimer Photon Machines laser ablation system at the Arizona LaserChron Center using the technique described in (Balica et al., 2020). Detrital sample 2PT10 was initially analyzed for detrital zircon U-Pb ages (n = 84) following protocols outlined in Gehrels et al. (2009). Of these 84 zircons, the Eocene-aged subset (n = 5) were targeted for spot-adjacent simultaneous U-Pb and trace element analysis. To increase the number of analyses of Eocene-aged zircons, additional grains from the same sample were targeted based on visual indicators using cathodoluminescence images acquired on a Hitachi S-3400 N scanning electron microscope with a Gatan Chroma Cl 2 attachment. Zircon standards Fish Canyon (28.5 Ma) and R33 (419.3 Ma) were used as age standards and Sri Lanka zircon was used as a trace element standard (Gehrels et al., 2009; Balica et al., 2020). Data and errors are presented in Table S5. Here we use the Eu anomaly ($Eu/Eu^* = Eu_N/[Sm_N * Gd_N]1/2$) of the zircons as a sensor for crustal thickness (Tang et al., 2020).

The application of geochemical data to estimate crustal thickness is based on the observation that the trace element signature of subduction-related magmas is correlated with certain crustal attributes (e.g., crustal thickness, Chiaradia, 2015). Specifically, the ratio of light to heavy rare earth elements (LREE and HREE, respectively, e.g., La/Yb) has been found to correlate with crustal thicknesses at global scales. This geochemical discrimination is possible as HREEs enter the liquid phase at low pressures, whereas at high pressures HREEs partition into garnet and/or amphibole (Hildreth and Moorbath, 1988). Conversely, LREEs are more abundant in thin arc residues (Kay and Mpodozis, 2002; Profeta et al., 2015). Thus, increasing ratios of whole rock La/Yb correlate with magmas that form at higher pressures and greater depths, and thus within thicker crust (Profeta et al., 2015). It is this relationship which we seek to replicate in the zircon accessory mineral phase. Within intermediate to felsic rocks, the Eu anomaly in zircons has been found to correlate with the whole rock La/Yb ratio (Tang et al., 2020; Profeta et al., 2015; Kay and Mpodozis, 2002). Other such geochemical proxies have also been recently calibrated (Chiaradia, 2015; Scott et al., 2018; Turner and Langmuir, 2015) demonstrating the applicability of this approach. As igneous rocks can be quite heterogenous, several tens of datapoints need to be averaged to obtain meaningful results (see Profeta et al., 2015, for protocol). Our new zircon crustal thickness estimates are compared to crustal thickness estimates calculated using published whole rock La/Yb ratios (Ramos et al., 1996).

Eu anomaly-based crustal thickness estimates were obtained from 41 zircon grains from the three ash samples (2PT170, 2PT152, and 2PT135), yielding a consistent median crustal thickness of ~40 km, which is slightly lower than but within error of values obtained from in situ whole rock data from the upper and lower Aconcagua Volcanic Complex units (Fig. 7A). Eu anomaly-based crustal thickness estimates were obtained for 12 Eocene zircons (40-47 Ma) from detrital sample 2PT10, yielding a median crustal thickness of ~35 km (Fig. 7A), which is a good baseline value for most of the Central Andes before significant crustal thickening. These Eu anomaly-based crustal thickness estimates agree with whole rock La/Yb ratios and associated crustal thickness estimates (Profeta et al., 2015) from measured zircon values using the partition coefficients determined by (Chapman et al., 2016) (Table S5).

## 7. Discussion and conclusions

The SMC indicates deposition by high-gradient alluvial fans in a wedge-top position within a structurally active, proximal thrust-belt setting while the Cerro Aconcagua stratovolcano was active between ca. 12 and 11 Ma. Of particular importance is the presence of growth strata in the SMC, which indicates active deformation of the Aconcagua fold-thrust belt at this time (Martos et al., 2022), whereas previous studies suggested quiescence and passive erosion (Giambiagi et al., 2015). This indicates that the Chilean, Precordillera and Aconcagua fold-thrust belts were active simultaneously during a period of arc magmatism at ~12-10 Ma, possibly during a regional high-flux magmatic event.

The paleo-crustal thickness calculations from Santa Maria Conglomerate comagmatic zircons indicate an average ~35 km thick crust ca. 38 Ma, and ~44 km thick crust ca. 12 Ma (Fig. 7A). Using the Profeta et al. (2015) correlations, published whole rock La/Yb values from arc rocks in the Farellones (32-33°S) and Teniente (34°S) areas, ca. 30 to 80 km SW of the study area; (Charrier et al., 2002; and references therein) suggests that the crust was ~35 km thick ca. 15 Ma and ~55 km just west of the Aconcagua region by ca. 6 Ma (Fig. 7A) as indicated by an abrupt change in La/Yb in the late Miocene (Kay et al., 2005). Insofar as modern crustal thickness is estimated to be ~55 km or more (Gans et al., 2011), our study indicates at least ~11 km of crustal thickening (Fig. 7) and ~2 km of elevation gain since ~12 Ma, assuming regional isostatic equilibrium and a reference crustal thickness of 35 km at sea level with values for mantle and crust densities of 3300 kg/m$^3$ and 2700 kg/m$^3$, respectively. This estimate is also consistent with paleoaltimetry data (Hoke et al., 2014a). The main crustal thickening events in the Aconcagua and 36°-34° regions occurred between ~15 and 12 Ma (Kay et al., 2005) and between ~12 and 6 Ma, during and after periods of active shortening (Fig. 6C). Peak magmatism at Aconcagua at ~12-10 Ma is consistent with a model whereby high-flux magmatism follows major shortening (~17-12; Giambiagi et al., 2015) and crustal thickening events but suggests shorter lag times (e.g., 7-2 My instead of 10-15 My sensu (DeCelles et al., 2015)) between the achievement of critical crustal thickness, crustal melting and high flux events. This history of deformation and magmatism does not require cyclical slab flattening and roll-back episodes (Kay et al., 2005; Ramos et al., 2014).

The history of crustal thickness observed at Aconcagua and in nearby regions to the south is significantly different from what is observed in the Central Andes to the north (at ca. 15-24°S) where crustal thicknesses of up to ~50 km were achieved by ~50 Ma and extreme crustal thicknesses (~70 km) by ~20 Ma (Fig. 7B; Chapman et al., 2015; Profeta et al., 2015). Combined with these earlier findings, our results suggest southward propagation of crustal thickening. We speculate that the excess crustal thickness in the Central Andes, to the north of our study area, may have provided a mechanism to drive southward crustal flow during the last ca. 20 Myr. Although axial lower crustal flow has been suggested to explain crustal thickness in the Central Andes (e.g., Ouimet and Cook, 2010), our study would suggest an opposite direction of crustal flow, from areas with thick crust in the Central Andes to areas with thinner crust to the south. Crustal anisotropy studies in the Bolivian Altiplano region suggest that weak middle crust may be flowing laterally, driven by the disequilibrium caused by lateral variations in crustal thickness (Lynner et al., 2018). Shortening in the AFTB during the last ~8 Ma is sufficient to produce a maximum crustal thickness of ~50 km (Giambiagi et al., 2015). In view

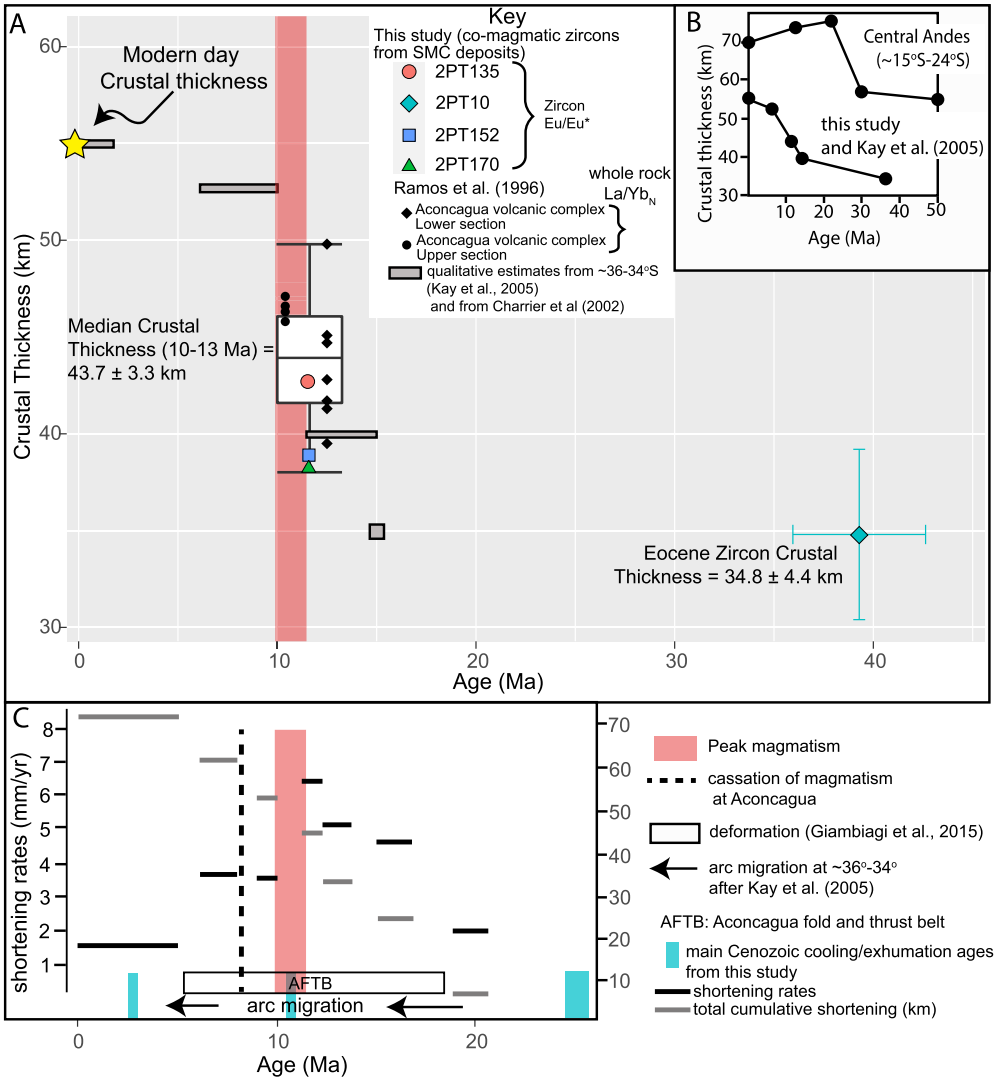


**Fig. 7.** A) Plot of crustal thickness estimates against age. Black symbols are crustal thickness estimates using La/Yb$_N$ from whole-rock data (WR) from samples from the lower and upper units of the Aconcagua Volcanic complex (Ramos et al., 1996) following Profeta et al. (2015). Crustal thickness using zircon Eu/Eu* (Eu$_N$/(Sm*Gd$_N$)1/2) was obtained following Tang et al. (2020). Crustal thickness estimates derived from Ramos et al. (1996) and this study at ~12-10 Ma were combined to produce a median crustal thickness estimate and associated 1$\sigma$ deviation. For sample 2PT10, only Eocene-aged zircons were used (Table S5). B) Crustal thickness estimates from Profeta et al. (2015). C) Shortening rates, estimates and deformation history from Giambiagi et al. (2015); arc migration history from Kay et al. (2005) based on the El Teniente area (for location see Fig. 1B).

of the fact that magmatism ceased by ~10 Ma at Cerro Aconcagua it is likely that the ~11 km of crustal thickening that has taken place since ca. 12 Ma (i.e., half of the total Cenozoic crustal thickening) was achieved by shortening. Although uncertainties in these calculations permit for shortening alone to account for the whole crustal thickening, if we accept these numbers at face value, they indicate a 5 km deficit (25% of the total Cenozoic crustal thickening of ~20 km) which could have been provided by crustal flow. We also note that these calculations do not account for any lithospheric removal.

This study shows that in the Aconcagua region shortening played an important role, accounting for at least half of the crustal thickening and uplift since mid-Miocene, including a time when the arc was active. This example demonstrates that active arc volcanism and a major fold-thrust belt can coexist spatially. The volume of surficial magmatic products (volcanic rocks) peaked while the fold-thrust belt was active. This has significant implications for how the local crustal "filter" influences the petrological evolution of Andean magmatic arcs (Ducea et al., 2015; Hildreth and Moorbath, 1988; Annen et al., 2006) and casts doubt on simplified arc models that call upon "mantle only" (Turner and Langmuir, 2015) followed by "basalt fractionation only" (Klein et al., 2021) mechanisms for making and diversifying sub-arc crust. For example, the classic (Plank and Langmuir, 1988) and more recent follow up paper by (Turner and Langmuir, 2015) predict that the thicker the crust, the lower the igneous flux of the magmatic arc (owing to less room for mantle melting), which is in direct contradiction with our example, showing that magmatism increased in volume as the crust was thickening, and with other studies showing that magmatic high flux events quickly follow or are synchronous with crustal thickening events (DeCelles et al., 2015; Ducea and Barton, 2007). Our work at Aconcagua indicates that the interplay between magmatism and shortening is complex and crustal shortening can dominate thickening even under the frontal arc region of a Cordilleran-type system. Further studies need to constrain material fluxes in and out of the arc crust at ideal locations where different components can be resolved, such as along the Aconcagua transect.

## CRediT authorship contribution statement

**Barbara Carrapa:** conceptualization, data collection, analysis, data interpretation, writing. **Peter G. DeCelles:** data collection, analysis, data interpretation, writing. **Mihai Ducea:** data interpretation, writing. **Gilby Jepson:** analysis, data interpretation, writing. **Arthur Osakwe:** analysis, data interpretation. **Elizabeth Balgord:** data interpretation, writing. **Andrea L. Stevens Goddard:** analysis, data interpretation, writing. **Laura Giambiagi:** data interpretation, writing.

## Declaration of competing interest

The authors declare that they have no known competing financial interests or personal relationships that could have appeared to influence the work reported in this paper.

## Acknowledgements

We acknowledge financial support from the National Geographic Society (9624-14) and NSF-FRES (EAR2020935). M.N.D. also acknowledges support from the Romanian Executive Agency for Higher Education, Research, Development and Innovation Funding project PN-III-P4-ID-PCCF-2016-0014. We are grateful to Dr. Rosemary Hickey-Vargas for handling this manuscript, Dr. Nicholas Perez and an anonymous reviewer for careful reviews that helped us to substantially improve the manuscript.

## Appendix A. Supplementary material

Supplementary material related to this article can be found online at https://doi.org/10.1016/j.epsl.2022.117526.

## References

Allmendinger, R., Jordan, T., Kay, S., Isacks, B., 1997. The evolution of the Altiplano-Puna Plateau of the Central Andes. Annu. Rev. Earth Planet. Sci. 25, 139–174.

Annen, C., Blundy, J.D., Sparks, R.S.J., 2006. The genesis of intermediate and silicic magmas in deep crustal hot zones. J. Petrol. 47, 505–539.

Balica, C., Ducea, M.N., Gehrels, G.E., Kirk, J., Roban, R.D., Luffi, P., Chapman, J.B., Triantafyllou, A., Guo, J., Stoica, A.M., Ruiz, J., Balintonia, I., Profeta, L., Hoffman, D., Petrescu, L., 2020. A zircon petrochronologic view on granitoids and continental evolution. Earth Planet. Sci. Lett. 531.

Beck, S.L., Zandt, G., Myers, S.C., Wallace, T.C., Silver, P.G., Drake, L., 1996. Crustal-thickness variations in the central Andes. Geology 24, 407–410.

Chapman, J.B., Ducea, M.N., DeCelles, P.G., Profeta, L., 2015. Tracking changes in crustal thickness during orogenic evolution with Sr/Y: an example from the North American Cordillera. Geology 43, 919–922.

Chapman, J.B., Gehrels, G.E., Ducea, M.N., Giesler, N., Pullen, A., 2016. A new method for estimating parent rock trace element concentrations from zircon. Chem. Geol. 439, 59–70.

Charrier, R., Baeza, O., Elgueta, S., Flynn, J.J., Gans, P., Kay, S.M., Munoz, N., Wyss, A.R., Zurita, E., 2002. Evidence for Cenozoic extensional basin development and tectonic inversion south of the at-slab segment, southern Central Andes, Chile (33o ± 36o S.L.). J. South Am. Earth Sci. 15, 117–139.

Chiaradia, M., 2015. Crustal thickness control on Sr/Y signatures of recent arc magmas: an Earth scale perspective. Sci. Rep. 5.

Cronin, S.J., Neall, V.E., Lecointre, J.A., Palmer, A.S., 1999. Dynamic interactions between lahars and stream flow: a case study from Ruapehu volcano, New Zealand. Geol. Soc. Am. Bull. 111, 28–38.

DeCelles, P.G., Gray, M., Ridgway, K., Cole, R., Pivnik, D., Pequera, N., Srivastava, P., 1991. Controls on synorogenic alluvial-fan architecture, Beartooth Conglomerate (Palaeocene), Wyoming and Montana. Sedimentology 38, 567–590.

DeCelles, P.G., Zandt, G., Beck, S., Currie, C.A., Ducea, M.N., Kapp, P., Gehrels, G.E., Carrapa, B., Quade, J., Schoenbohm, L.M., 2015. Cyclical orogenic processes in the Cenozoic Central Andes. In: DeCelles, P.G., Ducea, M.N., Carrapa, B., Kapp, P.A. (Eds.), Geodynamics of a Cordilleran Orogenic System: The Central Andes of Argentina and Northern Chile. In: Geological Society of America Memoir.

Ducea, M.N., Barton, M.D., 2007. Igniting flare-up events in Cordilleran arcs. Geology 35, 1047–1050.

Ducea, M.N., Paterson, S.R., DeCelles, P.G., 2015. High-volume magmatic events in subduction systems. Elements 11, 99–104.

Ganade, C.E., Lanari, P., Rubatto, D., Hermann, J., Weinberg, R.F., Basei, M.A.S., Tesser, L.R., Caby, R., Agbossoumondé, Y., Ribeiro, C.M., 2021. Magmatic flare-up causes crustal thickening at the transition from subduction to continental collision. Commun. Earth Environ. 41.

Gans, C.R., Beck, S.L., Zandt, G., Gilbert, H., Alvarado, P., Anderson, M., Linkimer, L., 2011. Continental and oceanic crustal structure of the Pampean flat slab region, western Argentina, using receiver function analysis: new high-resolution results. Geophys. J. Int., 45–58. https://doi.org/10.1111/j.1365-246X.2011.05023.x.

Gehrels, G., Rusmore, M., Woodsworth, G., Crawford, M., Andronicos, C., Hollister, L., Patchett, J., Ducea, M., Butler, R., Klepeis, K., Davidson, C., Friedman, R., Haggart, J., Mahoney, B., Crawford, W., Pearson, D., Girardi, J., 2009. U-Th-Pb geochronology of the Coast Mountains batholith in north-coastal British Columbia: constraints on age and tectonic evolution. Geol. Soc. Am. Bull. 121, 1341–1361.

Giambiagi, L., Tassara, A., Mescua, J., Tunik, M., Alvarez, P.P., Godoy, E., Hoke, G., Pinto, L., Spagnotto, S., Porras, H., Tapia, F., Jara, P., Bechis, F., García, V.H., Suriano, J., Moreiras, S.M., Pagano, S.D., 2015. Evolution of shallow and deep structures along the Maipo-Tunuyán transect (33°40′S): from the Pacific coast to the Andean foreland. In: Sepúlveda, S.A., Giambiagi, L.B., Moreiras, S.M., Pinto, L., Tunik, M., Hoke, G.D., Farías, M. (Eds.), Geodynamic Processes in the Andes of Central Chile and Argentina. In: Geological Society of London Special Publication.

Haschke, M., Siebel, W., Günter, A., Scheuber, E., 2002. Repeated crustal thickening and recycling during the Andean orogeny in north Chile (21oS-26oS). J. Geophys. Res. 107.

Hildreth, W., Moorbath, S., 1988. Crustal contributions to arc magmatism in the Andes of Central Chile. Contrib. Mineral. Petrol. 98, 455–489.

Hoke, G.D., Giambiagi, L.B., Garzione, C.N., Mahoney, J.B., Strecker, M.R., 2014a. Neogene paleoelevation of intermontane basins in a narrow, compressional mountain range, southern Central Andes of Argentina. Earth Planet. Sci. Lett. 506, 143–164.

Hoke, G.D., Graber, N., Mescua, J., Giambiagi, L., Fitzgerald, P., Matcalf, A.R., 2014b. Near pure surface uplift of the Argentine Frontal Cordillera: insights from (U–Th)/He thermochronometry and geomorphic analysis. In: Sepúlveda, S.A., Giambiagi, L.B., Moreiras, S.M., Pinto, L., Tunik, M., Hoke, G.D., Farías, M. (Eds.), Geodynamic Processes in the Andes of Central Chile and Argentina. Geological Society of London, London.

Horton, B.K., 2018. Tectonic regimes of the central and southern Andes: responses to variations in plate coupling during subduction. Tectonics 37, 402–429. https://doi.org/10.1002/2017TC004624.

Kay, S., Mpodozis, C., 2002. Magmatism as a probe to the Neogene Shallowing of the Nazca plate beneath the modern Chilean flat-slab. J. South Am. Earth Sci. 15, 39–57.

Kay, S.M., Godoy, E., Kurtz, A., 2005. Episodic arc migration, crustal thickening, subduction erosion, and magmatism in the south-central Andes. Geol. Soc. Am. Bull. 117, 67–88.

Klein, B.Z., Jagoutz, O., Ramezani, 2021. High-precision geochronology requires that ultrafast mantle-derived magmatic fluxes built the transcrustal Bear Valley Intrusive Suite, Sierra Nevada, California, USA. Geology 49, 106–110.

Ludwig, K., Mundil, R., 2002. Extracting reliable U-Pb ages and errors from complex populations of zircons from Phanerozoic tuffs. Geochim. Cosmochim. Acta 66.

Lynner, C., Beck, S.L., Zandt, G., Porritt, R.W., Lin, F.-C., Eilon, Z.C., 2018. Midcrustal deformation in the Central Andes constrained by radial anisotropy. J. Geophys. Res., Solid Earth.

Mackaman-Lofland, C., Horton, B.K., Fuentes, F., Constenius, K.N., Stockli, D.F., 2019. Mesozoic to Cenozoic retroarc basin evolution during changes in tectonic regime, southern Central Andes (31–33°S): insights from zircon U-Pb geochronology. J. South Am. Earth Sci., 289–318. https://doi.org/10.1016/j.jsames.2018.10.004.

Martos, F.E., Naipauer, M., Fennell, L.M., Acevedo, E., Hauser, N., Folguera, A., 2022. Neogene evolution of the Aconcagua fold-and-thrust belt: linking structural, sedimentary analyses and provenance U-Pb detrital zircon data for the Penitentes basin. Tectonophysics 825.

McQuarrie, N., 2002. The kinematic history of the central Andean fold-thrust belt, Bolivia: implications for building a high plateau. Geol. Soc. Am. Bull. 114, 950–963.

Miall, A.D., 2006. The Geology of Fluvial Deposits, Sedimentary Facies, Basin Analysis, and Petroleum Geology, 4th edition. Springer-Verlag, Berlin.

Nemec, W., Steel, R.J., 1984. Alluvial and coastal conglomerates: their significant features and some comments on gravelly mass-flow deposits. In: Can. Soc. Pet. Geol. Memoir.

Ouimet, W.B., Cook, K.L., 2010. Building the central Andes through axial lower crustal flow. Tectonics 29.

Pepper, M., Gehrels, G., Pullen, A., Ibanez-Mejia, M., Ward, K.M., Kapp, P., 2016. Magmatic history and crustal genesis of western South America: constraints from U-Pb ages and Hf isotopes of detrital zircons in modern rivers. Geosphere 12.

Plank, T., Langmuir, C.H., 1988. Tracing trace elements from sediment input to volcanic output at subduction zones. Nature 362, 739–743.

Profeta, L., Ducea, M.N., Chapman, J.B., Paterson, S.R., Gonzales, S.M.H., Kirsch, M., Petrescu, L., DeCelles, P.G., 2015. Quantifying crustal thickness over time in magmatic arcs. Sci. Rep. 5.

Quade, J., Dettinger, M.P., Quade, J., Carrapa, B., DeCelles, P.G., Murray, K.E., Huntington, K.W., Cartwright, A., Canavan, R.R., Gehrels, G., Clementz, M., 2015. The growth of the central Andes, 22°S–26°S. In: Geological Society of America Memoir, vol. 12.

Ramos, V.A., 2009a. Darwin at Puente del Inca: observations on the formation of the Inca's bridge and mountain building. Rev. Asoc. Geol. Argent. 64 (1), 170–179.

Ramos, V.A., 2009b. Anatomy and global context of the Andes: main geologic features and the Andean orogenic cycle. In: Backbone of the Americas: Shallow Subduction, Plateau Uplift, and Ridge and Terrane Collision, vol. 204, pp. 31–65.

Ramos, V.A., Kay, S.M., Perez, D.J., 1996. El volcanismo de la region del Aconcagua. In: Ramos, V.A., Aguirre-Urreta, M.B., Alvarez, P.P., Cegarra, M.I., Cristallini, O.C., Kay, S.M., Lo Forte, G.L., Pereyra, F.X., Perez, D.J. (Eds.), Geologia de la region del Aconcagua. Subsecreteria de Mineria de la nacion direccion national del servicio geologico, Buenos Aires, pp. 297–316.

Ramos, V.A., Litvak, V.D., Folguera, A., Spagnuolo, M., 2014. An Andean tectonic cycle: from crustal thickening to extension in a thin crust (34°-37°S). Geosci. Front. 5, 351–367.

Riesner, M., Simoes, M., Carrizo, D., Lacassin, R., 2019. Early exhumation of the Frontal Cordillera (Southern Central Andes) and implications for Andean mountain-building at ∼33.5°S. Sci. Rep.

Scott, E.M., Allen, M.B., Macpherson, C.G., McCaffrey, K.J.W., Davidson, J.P., Saville, C., Ducea, M.N., 2018. Andean surface uplift constrained by radiogenic isotopes of arc lavas. Nat. Commun.

Smith, G.A., 1986. Coarse-grained nonmarine volcaniclastic sediment: terminology and depositional process. Geol. Soc. Am. Bull. 97, 1–10.

Smith, G.A., Lowe, D.R., 1991. Lahars: volcano-hydrologic events and deposition in the debris flow—hyperconcentrated flow continuum. In: Fisher, R.V., Smith, G.A. (Eds.), Sedimentation in Volcanic Settings. SEPM Society for Sedimentary Geology.

Sruogaa, P., Llambías, E.J., Fauqué, L., Schonwandtc, D., Repol, D.G., 2005. Volcanological and geochemical evolution of the Diamante Caldera–Maipo volcano complex in the southern Andes of Argentina (34°10′S). J. South Am. Earth Sci. 19, 399–414.

Stevens Goddard, A.L., Carrapa, B., 2017. Using basin thermal history to evaluate the role of Miocene–Pliocene flat-slab subduction in the southern Central Andes (27° S–30° S). Basin Res.

Tang, M., Ji, W.-Q., Chu, X., Wu, A., Chen, C., 2020. Reconstructing crustal thickness evolution from europium anomalies in detrital zircons. Geology 49, 76–80.

Turner, S.J., Langmuir, C.H., 2015. What processes control the chemical compositions of arc front stratovolcanoes? Geochem. Geophys. Geosyst. 16, 1865–1893.

Vicente, J.-C., Leanza, H.A., 2009. El Frente de Corrimiento andino al nivel de Los Cerros Penitentes y visera (Alta Cordillera de Mendoza): aspectos cronologicos y cartograficos. Rev. Asoc. Geol. Argent. 65, 97–110.